Relationship Between the Western Pacific Subtropical High and the Subtropical East Asian Diabatic Heating During South China Heavy Rains in June 2005*

WANG Lijuan† (王黎娟), GAO Hui (高 辉), GUAN Zhaoyong (管兆勇), and HE Jinhai (何金海)

Key Laboratory of Meteorological Disaster of Ministry of Education, College of Atmospheric Sciences, Nanjing University of Information Science & Technology, Nanjing 210044

(Received July 11, 2010)

ABSTRACT

Based on the daily NCEP/NCAR reanalysis data, the position variation of the western Pacific subtropical high (WPSH) in June 2005 and its relation to the diabatic heating in the subtropical East Asia are analyzed using the complete vertical vorticity equation. The results show that the position variation of the WPSH is indeed associated with the diabatic heating in the subtropical East Asian areas. In comparison with June climatology, stronger heating on the north side of the WPSH and relatively weak ITCZ (intertropical convergence zone) convection on the south side of the WPSH occurred in June 2005. Along with the northward movement of the WPSH, the convective latent heating extended northward from the south side of the WPSH. The heating to the west of the WPSH was generally greater than that inside the WPSH, and each significant enhancement of the heating field corresponded to a subsequent westward extension of the WPSH. In the mid troposphere, the vertical variation of heating on the north of the WPSH was greater than the climatology, which is unfavorable for the northward movement of the WPSH. On the other hand, the vertical variation of heating south of the WPSH was largely smaller than the climatology, which is favorable for the anomalous increase of anticyclonic vorticity, leading to the southward retreat of the WPSH. Before the westward extension of the WPSH in late June 2005, the vertical variation of heating rates to (in) the west (east) of the WPSH was largely higher (lower) than the climatology, which is in favor of the increase of anticyclonic (cyclonic) vorticity to (in) the west (east) of the WPSH, inducing the subsequent westward extension of the WPSH. Similar features appeared in the lower troposphere. In a word, the heating on the north–south, east–west of the WPSH worked together, resulting in the WPSH extending more southward and westward in June 2005, which is favorable to the maintenance of the rainbelt in South China.

Key words: heavy rains in South China, western Pacific subtropical high, diabatic heating, complete vertical vorticity equation

Citation: Wang Lijuan, Gao Hui, Guan Zhaoyong, et al., 2011: Relationship between the western Pacific subtropical high and the subtropical East Asian diabatic heating during South China heavy rains in June 2005. *Acta Meteor. Sinica*, **25**(2), 203–210, doi: 10.1007/s13351-011-0027-6.

1. Introduction

In June 2005, large-scale intense rainfall events occurred successively in the southern Jiangnan area and much of South China. Parts of Guangxi, Guangdong, Fujian, Jiangxi, Hunan, and Zhejiang provinces were hit by torrential rains and even exceptionally heavy rains in some local areas. These events resulted in flooding and landslide, leading to considerable casualties and loss of property. In particular, during June 17–26, a persistent and strong rainfall episode took place in South China and the east of Jiangnan area characterized by an extensive area and high severity with precipitation of 100–200 mm in general and the maxium value of 400–1100 mm. Overall, 100–300-mm higher than normal rainfall was observed in South China.

In June 2005, the western Pacific subtropical high (WPSH) was more southward and westward than normal, allowing the confluence over the South China Sea

*Supported by the National Natural Science Foundation of China (40975057), National Key Technology R&D Program (2007BAC29B02 and 2009BAC51B01), Ph.D. Program Fund of the Ministry of Education of China (20093228120001), and Qing Lan Project of Jiangsu Province.

†Corresponding author: wljfw@163.com.

(Chinese version published in Vol. 67, No. 4, 667–673, 2009)

of easterly flows from the south side of the WPSH with the southwesterly warm and moist flows from the equatorial Indian Ocean and the Bay of Bengal. Both branches of airflows transported plenty of water vapor into South China and the Jiangnan area along the west side of the WPSH. The center of strong water vapor convergence was located in South China, which led to the occurrence and maintenance of torrential rains (Wang et al., 2007; Xiong et al., 2007).

Many meteorologists suggested that the flood/drought in South China is closely associated with the seasonal shift of the WPSH (Huang, 1963; Wu and Chou, 2002; Lu, 2001; Shu and Luo, 2003). In particular, the zonal location and the north-south movement of the WPSH are responsible for the establishment of the East Asian summer monsoon and precipitation over the Yangtze River valley and South China (Liu and Wu, 2000). As a primary component of the East Asian monsoon system, the WPSH is closely related to diabatic heating, and its zonal and meridional shifts, are due to a large extent to the spatial patterns of diabatic heating (Huang and Li, 1988). Wu et al. (1999b) and Liu et al. (1999a, b) also pointed out that the latent heating of condensation induced by the East Asian monsoon precipitation plays a key role in changing the WPSH location and intensity. The WPSH and the East Asian summer monsoon rainfall interact with each other.

In this study, through comparison with the long-term mean, variations of the WPSH position during heavy rains over South China in June 2005 are analysed, and the influence of the diabatic heating on the activity of the WPSH is investigated by using the complete vertical vorticity equation (Wu et al., 1999a). This study aims to provide a better understanding of the physical mechanisms for floods in South China related to the shift of the WPSH position, and to better predict the flood/drought in this region.

2. Data and method

The primary data used in this study are: (1) the daily National Centers for Environmental Prediction/National Center of Atmospheric Research (NCEP/NCAR) reanalysis data with a 2.5°×2.5° horizontal resolution; and (2) WPSH ridge line index data from the National Climate Center (NCC) of China.

2.1 Calculation of heat source

Atmospheric heat source is calculated according to Yanai et al. (1973):

$$Q_1 = c_p(\frac{\partial \overline{T}}{\partial t} + \boldsymbol{V}\cdot\bigtriangledown\overline{T} + \overline{\omega}(\frac{p}{p_0})^{\kappa}\frac{\partial\overline{\theta}}{\partial p}), \quad (1)$$

where $\kappa = R/c_p$, R and c_p are the gas constant for dry air and specific heat at constant pressure, respectively, and θ is the potential temperature. The three terms in the right brackets describe local variation, horizontal advection and vertical transport, respectively. Q_1 denotes the heating rate per unit time and air mass.

Equation (1) can be rewritten as:

$$Q_1 = Q_R + L(\overline{c} - \overline{e}) - \frac{\partial}{\partial p}(\overline{S'\omega'}). \quad (2)$$

Integrating both sides of Eq. (2) from $p_{\rm t}$ (100 hPa) to $p_{\rm s}$ (surface pressure), we obtain

$$\langle Q_1\rangle = \langle Q_{\rm R}\rangle + E_{\rm L} + H_{\rm S}, \quad (3)$$

where $\langle\ \rangle = \frac{1}{g}\int_{p_{\rm t}}^{p_{\rm s}}()\ {\rm d}p$. It can be seen that the atmospheric apparent heat source $\langle Q_1\rangle$ consists of radiative heating (cooling) $\langle Q_{\rm R}\rangle$, latent heating from precipitation $E_{\rm L}$, and surface sensible heat flux $H_{\rm S}$.

2.2 The complete vertical vorticity equation

The complete vertical vorticity equation (Wu et al., 1999a) can be written as

$$\frac{\partial\zeta}{\partial t} + \boldsymbol{V}\cdot\bigtriangledown\zeta + \beta v = (1-\kappa)(f+\zeta)\frac{\omega}{P} -(f+\zeta)\frac{Q}{\theta} + \frac{1}{\alpha}\frac{\rm d}{{\rm d}t}\Big(\frac{P_{\rm E}}{\theta_z} - C_d\Big) + \frac{1}{\theta_z}F_\zeta\cdot\bigtriangledown\theta_z + \frac{f+\zeta}{\theta_z}\frac{\partial Q}{\partial z} - \frac{1}{\theta_z}\frac{\partial v}{\partial z}\frac{\partial Q}{\partial x} + \frac{1}{\theta_z}\frac{\partial u}{\partial z}\frac{\partial Q}{\partial y},\quad \theta_z \neq 0, \quad (4)$$

where $\theta_z = \partial\theta/\partial z$, $P_{\rm E}$ is Ertel geopotential vorticity, C_d is the parameter representing atmospheric thermal structure, and others are meteorological symbols in common use. Respectively, the first four terms on the right-hand side represent contributions from the vertical motion, heating source, internal thermodynamics variation in the atmosphere, and frictional dissipation to the vorticity variation; the last three terms on the right-hand side are contributions from spatial inhomogeneous heating.

Taking no account of the effects of internal thermodynamics variation in the atmosphere, heating source, and frictional dissipation, but only the effects of the apparent heat source Q_1 and vertical motion, Eq. (4) becomes

$$\frac{\partial\zeta}{\partial t}+\boldsymbol{V}\cdot\nabla\zeta+\beta v=(f+\zeta)(1-\kappa)\frac{\omega}{P}+\frac{f+\zeta}{\theta_z}\frac{\partial Q_1}{\partial z}-\frac{1}{\theta_z}\frac{\partial v}{\partial z}\frac{\partial Q_1}{\theta x}-\frac{1}{\theta_z}\frac{\partial u}{\partial z}\frac{\partial Q_1}{\partial y}. \quad (5)$$

From the scale analysis (Wu et al., 1999b), the vertical motion and horizontal inhomogeneous heating induced by the atmospheric apparent heating source are at 10^{-11}–10^{-12} order of magnitude, which is one order of magnitude or more smaller than the forcing by the vertical variation of the apparent heat source (10^{-10}). Then, Eq. (5) is changed into

$$\frac{\partial\zeta}{\partial t}+\boldsymbol{V}\cdot\nabla\zeta+\beta v=\frac{f+\zeta}{\theta_z}\frac{\partial Q_1}{\partial z}. \quad (6)$$

In the Northern Hemisphere, $f=2\Omega\sin\phi$, which is always larger than zero and increases with latitude. Generally, $f+\zeta\geqslant 0$, $\theta_z=\partial\theta/\partial z$ is also positive in large-scale motion.

3. Characteristics of the WPSH in June 2005

Figure 1 shows the position of the 5880-gpm contour at 500-hPa during 17–26 June 2005 and its climatological mean in June. It is obvious that the WPSH in 2005 was distributed along a west-east zone, spanning about 20 latitudes, with the 120°E ridge line staying around 16°N and the westmost ridge point around 110°E. Compared with the climatological mean, the WPSH ridge in 2005 shifted southward about 6 latitudes and the westmost ridge point extended westward about 20 longitudes. Confluence of mid-latitude northwesterly flows with southwesterly on the north side of the WPSH controlled most parts of South China. The above WPSH anomalies may have caused the flood over South China in June 2005.

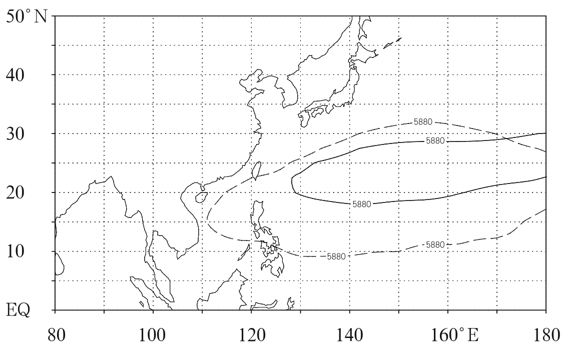

Fig. 1. The position of the 5880-gpm contour (dashed line) at 500 hPa during 17–26 June 2005 and its climatological mean in June (solid line).

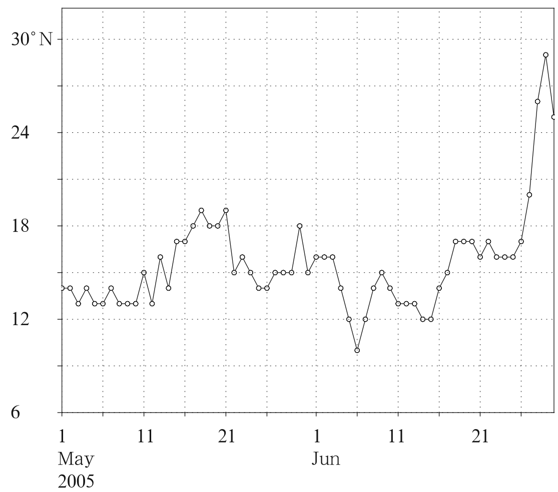

Fig. 2. Temporal evolution of the ridge (120°E) of the WPSH during May–June 2005.

Figure 2 depicts the temporal evolution of the WPSH ridge line along 120°E during May–June 2005. We see that the ridge line took on a more southern position compared to normal. During 3–6 June, the ridge retreated from 16°N to the south of 12°N, followed by its gradual northward shlifting to 15°N and re-withdrawal from 9 June, residing around 12°N on 15 June. Another northward shift began from 16–25 June, with the ridge line remaining stagnant at 16°–17°N, which was responsible for the long lasting rainband in South China, with concentrated and persistent heavy rains. The WPSH made another northward jump on 26 June, leading to the beginning of the Meiyu rainfall in the Yangtze River valley, with the ridge line crossing 24°N on 28 June. When the WPSH ridge line was located to the south of 20°N, warm and moist airflows carried by the WPSH met in South China with weak and cold air moving southward from midlatitudes, forming a frontal zone and thereby generating a stable rainband.

4. Horizontal distributions of the diabatic heating in the subtropical East Asia

Complex interactions exist between the WPSH and the convective heating on its north/south and east/west sides. Based on the complete vertical vorticity tendency equation, by scale analyses and numerical simulations, Wu et al. (1999a, b) and Liu et al. (1999a, b) suggested that the condensational latent heating played an important role in the summertime location and intensity of the Eastern Hemispheric WPSH. This section will focus on the effects of the diabatic heating induced by convections on the WPSH in June 2005 and the difference in the heating from the climatological mean.

Figure 3 shows the WPSH shifts along the north-south direction in June. As for the climatological mean (Fig. 3a), there is strong heating south of the WPSH throughout the year, which is stronger than that north of the WPSH due to continuous convective development in the intertropical convergence zone (ITCZ). The heating north of the WPSH changes with the WPSH seasonal northward movement. In early June, the WPSH withdraws eastward with a weak ridge in its western portion and approaches to the east of 130°E after the summer monsoon onset, and convection develops in the west of the WPSH (120°–130°E), leading to the weak heating over the WPSH region (120°–150°E). In mid June, along with the WPSH northward movement, the WPSH is situated in a cooling environment where radiative cooling and upward sensible heating are dominant. The subtropical monsoon rainband produces heating on the north of the WPSH, where $\langle Q_1 \rangle$ increases significantly. It is noted that the contour of 5880 gpm appears during this period, suggesting that the WPSH reaches the strongest. The area encircled by the 5880-gpm contour corresponds to the descending cloudless region, which is thus surrounded by the zero heating contour.

Different from the climatology, the WPSH ridge is steadily maintained at the south of 15°N during early June 2005 (Fig. 3b). There was strong heating on the north of the WPSH while the heating associated with the ITCZ convection was weak. The WPSH jumped northward on 11 June and its ridge line remained at about 22°N from 16 to 26 June, which was favorable for the rainbelt staying in South China. At the same time, $\langle Q_1 \rangle$ increased remarkably on the north of the WPSH. The WPSH moved northward again on 26 June. It is noted that the heating south of the WPSH extended northward as the WPSH shifted northward (as shown by the arrows in Fig. 3b). The similar feature can be found during the Meiyu rainfall in 1998 (Wang et al., 2006).

Figure 4 shows the east-west shifts of the WPSH in June. The climatological southern boundary of the WPSH advances continuously from 15° to 20°N, with convection developing south of the WPSH, corresponding to the weak heating in the WPSH area

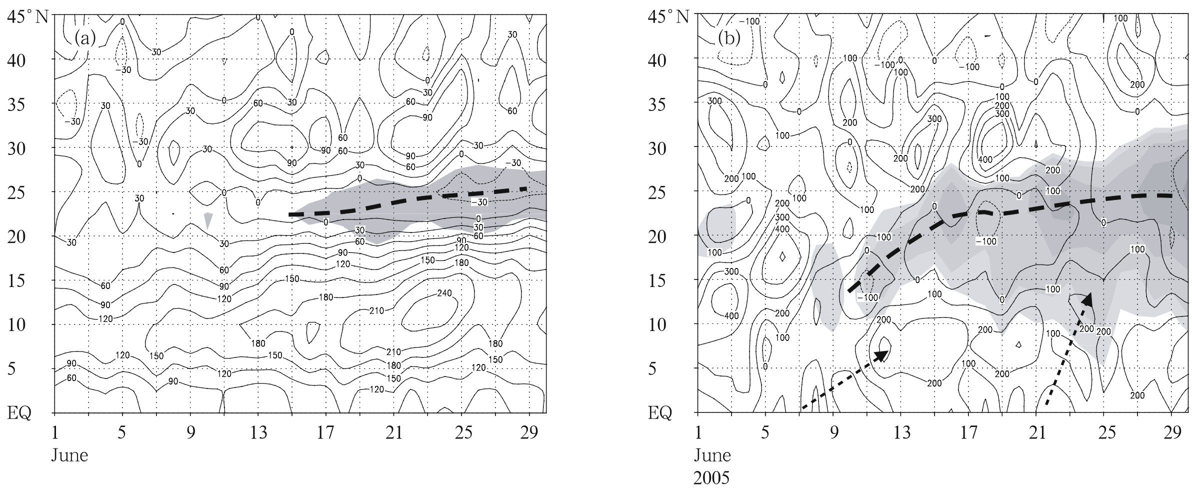

Fig. 3. Time-latitude cross-sections of the atmospheric apparent heat source $\langle Q_1 \rangle$ (W m^{-2}) over 120°–150°E for (a) June climatological mean and (b) June 2005. Shadings indicate areas with 500-hPa geopotential height greater than 5880 gpm, and thick dashed lines represent mean locations of the WPSH ridge. Dot-shafted arrows denote the maximum value axes of $\langle Q_1 \rangle$, which correspond to the northward advances of the WPSH.

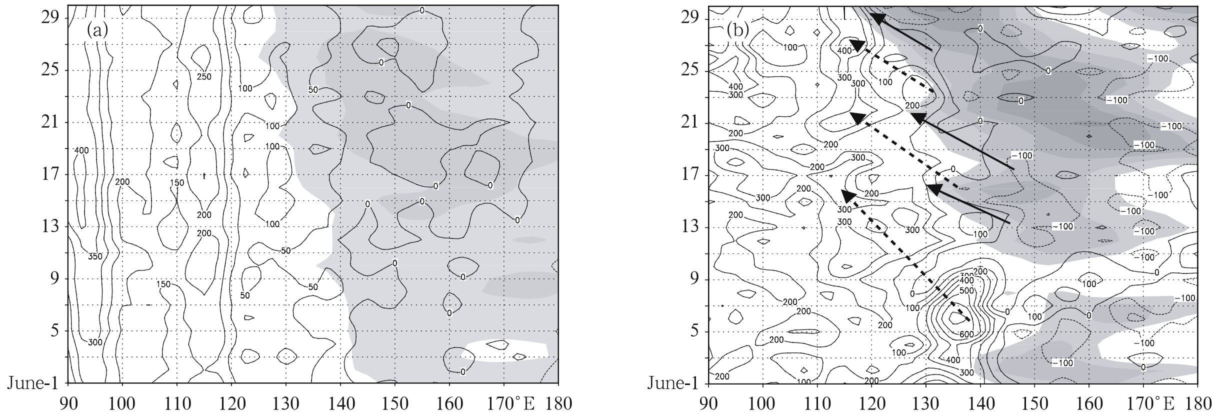

Fig. 4. Time-longitude cross-sections of the average atmospheric apparent heat source $\langle Q_1 \rangle$ over 15°–30°N (unit: W m^{-2}) for (a) June climatological mean and (b) June 2005. Shadings indicate areas with 500-hPa geopotential height greater than 5870/5880 gpm in (a/b). Dot-shafted arrows denote the maximum value axes of $\langle Q_1 \rangle$ and solid shafted arrows delineate the westward extensions of the WPSH.

at 15°–30°N. The areas surrounded by the 5880-gpm contour are in agreement with the zero line of heating (Fig. 4a). In comparison with the climatology, the WPSH extended westward thrice in June 2005 (Fig. 4b). In early June, the westmost ridge point of the WPSH was located east of 140°E. From 11 to 16 June, the WPSH extended westward to 130°E, then retreated eastward rapidly and stretched again to the west of 130°E around 21 June. The WPSH extended westward the third time to the west of 115°E around 26 June, in conjunction with the northward movement of the WPSH. It is noted that the high-value heating centers to the west of the WPSH were followed by the westward extension of the WPSH. In general, the relatively weak heating in the WPSH area was surrounded by the 5880-gpm contour and the WPSH center was usually a cooling area.

5. Effects of the vertical variation of diabatic heating on the WPSH

5.1 Meridional Effect

On the south/north side of the WPSH (south: 10°–15°N, 110°–150°E; north: 30°–35°N, 110°–150°E), easterly (westerly) prevails ($v \approx 0$), and vorticity advection along x axis is quite weak. Thus, from Eq. (6), we obtain

$$\frac{\partial \zeta}{\partial t} \propto \frac{f+\zeta}{\theta_z}\frac{\partial Q_1}{\partial z}. \quad (7)$$

The weak cooling in the center of the WPSH is associated with radiative cooling due to clear sky. On the north and south of the WPSH, the heating rates peak at 500 hPa (Wen and He, 2002). Thus, the peak height (at about 450 hPa) divides the troposphere into upper and lower layers. In the lower layer, $\frac{f+\zeta}{\partial z}\frac{\partial Q_1}{\partial \theta_z} > 0$, so $(\frac{\partial \zeta}{\partial t})_{Q_1} > 0$; while in the upper layer, $\frac{f+\zeta}{\theta_z}\frac{\partial Q_1}{\partial z} < 0$, so $(\frac{\partial \zeta}{\partial t})_{Q_1} < 0$. Thereby, the heating induced by convective precipitation on the north of the WPSH is favorable for the development of lower-layer cyclonic vorticity that depresses the WPSH northward movement, and also favorable for the increase of upper-layer anticyclonic vorticity that helps the WPSH northward movement. This leads to a polarward slope of the WPSH ridge axis with height. In contrast, the heating on the south side produces lower-layer cyclonic vorticity (upper-layer anticyclonic vorticity) that helps the WPSH northward (southward) migration, resulting in an equatorward slope of the WPSH ridge axis with height. In this sense, the meridional movement of the WPSH depends on the relative magnitude of vertical change of diabatic heating on the north/south side of the WPSH. When the heating rate on the south side is greater than that on the north, this is in favor of the WPSH northward shift, and vice versa.

Figures 5a and 5b show daily evolution of average

$\frac{f+\zeta}{\theta_z}\frac{\partial Q_1}{\partial z}$ on the north and south sides of the WPSH at 500 hPa for June climatological mean and June 2005, respectively. It is seen that the vertical variation of heating on the north side of the WPSH in June 2005 was generally greater than the climatological mean, i.e., $(\frac{f+\zeta}{\theta_z}\frac{\partial Q_1}{\partial z})_{2005} > (\frac{f+\zeta}{\theta_z}\frac{\partial Q_1}{\partial z})_{\rm mean} > 0$, so $(\frac{\partial\zeta}{\partial t})_{2005} > 0$, which was unfavorable for the northward movement of the WPSH; whereas, on the south side, $\left(\frac{f+\zeta}{\theta_z}\frac{\partial Q_1}{\partial z}\right)_{2005} < 0 < \left(\frac{f+\zeta}{\theta_z}\frac{\partial Q_1}{\partial z}\right)_{\rm mean}$, so $\left(\frac{\partial\zeta}{\partial t}\right)_{2005}$ <0, which was favorable for the increase of anticyclonic vorticity and WPSH southward movement. With the effects of the diabatic heating on both north and southsides, the WPSH extended more southward in June 2005 (Fig. 1).

5.2 Zonal effect

In this section, we will discuss the effect of vertical variation of diabatic heating to (in) the west (east) of WPSH on its zonal movements.

Assume $u \approx 0$ around the ridge line, advection is small and consider only longer time scales, the local variation item $\frac{\partial\zeta}{\partial t}$ can be neglected. From Eq. (6), we obtain:

$$\beta v \propto \frac{f+\zeta}{\theta_z}\frac{\partial Q_1}{\partial z}. \quad (8)$$

In the climatological mean, the diabatic heating is mainly concentrated in the mid troposphere to/on the west and east sides of the WPSH (Wen and He, 2002). To the west side, if $\frac{f+\zeta}{\theta_z}\frac{\partial Q_1}{\partial z} > 0$, then $\beta v > 0$, which leads to the southerly enhancement, inducing the anticyclonic circulation on the east side of the heating source at 500 hPa and favorable for the WPSH maintenance and westward extension.

Figure 6a shows daily evolution of average $\frac{f+\zeta}{\theta_z}\frac{\partial Q_1}{\partial z}$ to (on) the west (east) side of WPSH at 500 hPa for June climatological mean and June 2005. It is found that the vertical variation of diabatic heating to the west side of the WPSH was generally higher than the climatological mean before the WPSH extended westward on June 21 and 26, i.e., $(\frac{f+\zeta}{\theta_z}\frac{\partial Q_1}{\partial z})_{2005} > 0 > (\frac{f+\zeta}{\theta_z}\frac{\partial Q_1}{\partial z})_{\rm mean}$, which was favorable for the increase of anticyclonic vorticity in the east of the heating area (to the west side of the WPSH), inducing the subsequent westward extension of the WPSH. This result is in agreement with the above discussion that heating enhancement is followed by the WPSH westward extension.

On the east side of the WPSH, the vertical change of diabatic heating was generally lower than the climatological mean during June (Fig. 6b). Namely, $(\frac{f+\zeta}{\theta_z}\frac{\partial Q_1}{\partial z})_{2005} < 0 < (\frac{f+\zeta}{\theta_z}\frac{\partial Q_1}{\partial z})_{\rm mean}$, which leads to the increase of cyclonic vorticity on the east side of the heating source, and favors the WPSH westward

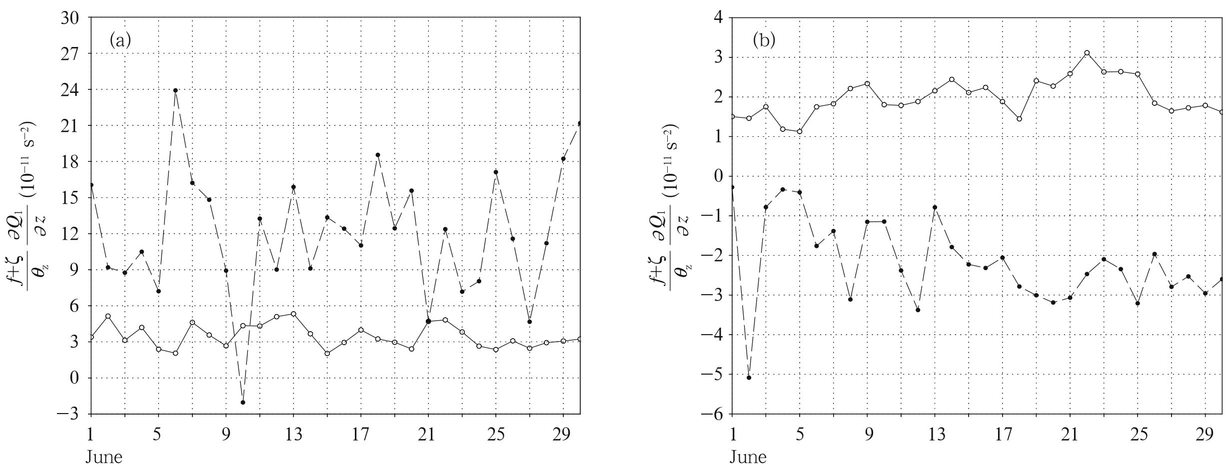

Fig. 5. Daily evolution of $\frac{f+\zeta}{\theta_z}\frac{\partial Q_1}{\partial z}$ (unit: 10^{-11} s^{-2}) on the north (a; 30°–35°N, 110°–150°E) and south sides (b; 10°–15°N, 110°–150°E) of the WPSH at 500 hPa for June climatological mean (solid line) and June 2005 (dashed line).

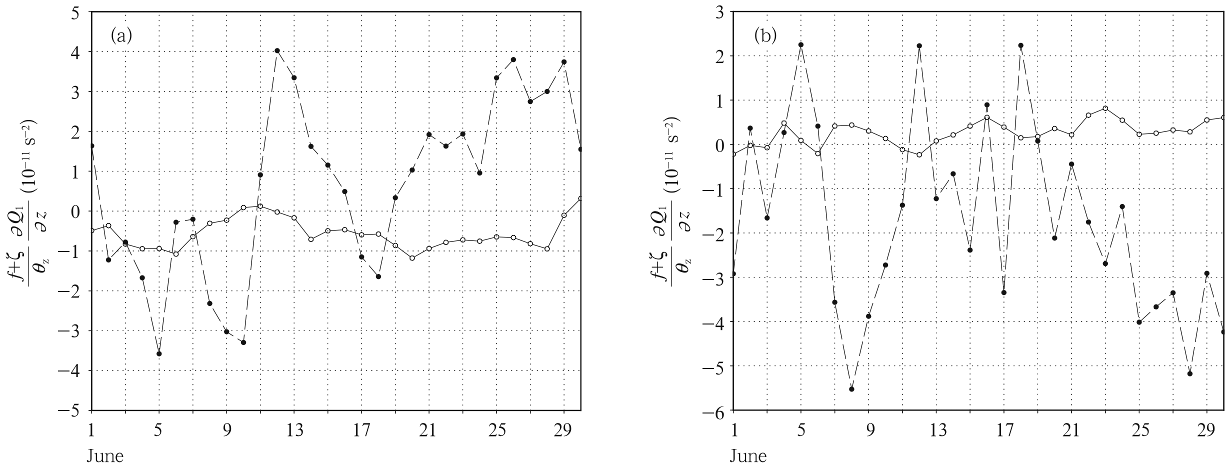

Fig. 6. Daily evolution of average $\frac{f+\zeta}{\theta_z}\frac{\partial Q_1}{\partial z}$ (unit: 10^{-11} s^{-2}) to the west (a; 15°–30°N, 60°–110°E) and on the east sides (b; 15°–30°N, 120°–170°E) of the WPSH at 500 hPa for June climatological mean (solid line) and June 2005 (dashed line).

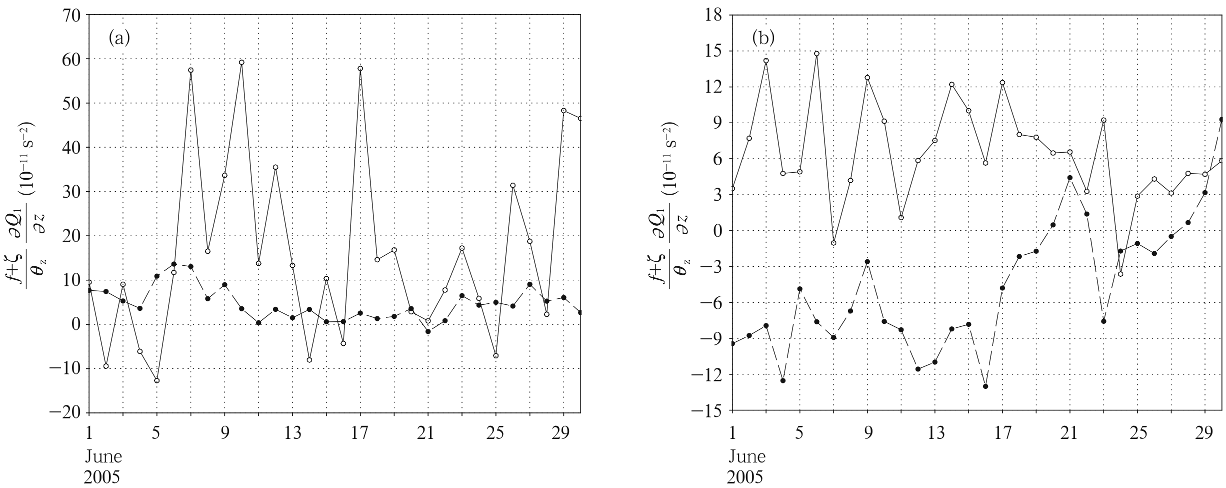

Fig. 7. Daily evolution of average $\frac{f+\zeta}{\theta_z}\frac{\partial Q_1}{\partial z}$ (unit: 10^{-11} s^{-2}) (a) on the north (30°–35°N, 110°–150°E; solid line) and south (10°–15°N, 110°–150°E; dashed line) sides, and (b) to the west (15°–30°N, 60°–110°E; solid line) and on the east (15°–30°N, 120°–170°E; dashed line) sides of the WPSH at 850 hPa in June 2005.

extension.

Some studies (Hoskins, 1996; Lu, 2002) indicate that the diabatic heating in the lower troposphere has a significant influence on the WPSH (or vorticity). From Fig. 7, we can see that $\frac{f+\zeta}{\theta_z}\frac{\partial Q_1}{\partial z}$ on the north side of the WPSH was generally greater than that on the south side, and $\frac{f+\zeta}{\theta_z}\frac{\partial Q_1}{\partial z}$ to the west of the WPSH was higher than that in the east. This suggests that greater vertical variation of diabatic heating on the north side of WPSH favored its southward retreat, and higher vertical variation of diabatic heating to the west side favored its westward extension.

6. Conclusions and discussion

(1) The variation of the WPSH position is associated with the diabatic heating in subtropical East Asia. In comparison with the climatology, there was strong heating on the north side of the WPSH and relatively weak ITCZ convection on the south side of the WPSH in June 2005. The latent heating on the

south side extended northward along with the WPSH northward jumping.

(2) The heating to the west of the WPSH was generally greater than that in the WPSH areas in June 2005. The significantly enhanced heating to the west of the WPSH was followed by the westward extension of the WPSH.

(3) The vertical variation of heating on the north(south) of the WPSH during June 2005 was generally greater (smaller) than the climatology, which was unfavorable (favorable) for the northward (southward) movement of the WPSH. In the lower troposphere, the vertical variation of heating on the north of the WPSH was greater than that on the south. Therefore, with the effects of both north- and south-side diabatic heating, the WPSH migrated more southward in June 2005.

(4) The vertical variation of heating to (in) the west (east) of the WPSH before late June 2005 was generally greater (smaller) than the climatology, which was favorable for the increase of anticyclonic (cyclonic) vorticity to (on) the west (east) side of the WPSH, inducing the subsequent westward extension of the WPSH. In the lower troposphere, the vertical variation of heating to the west of the WPSH was greater than that in the east. Therefore, with the effects of both west- and east-side diabatic heating, the WPSH extended more westward in June 2005.

REFERENCES

Hoskins, B., 1996: On the existence and strength of the summer subtropical anticyclones. *Bull. Amer. Meteor. Soc.*, **77**(6), 1287–1292.

Huang Ronghui and Li Weijing, 1988: The effects of heat source anomalies over the tropical western Pacific in summer on the subtropical high over East Asia and its physical mechanisms. *Chinese J. Atmos. Sci.*, **12**(Special Issue), 107–116. (in Chinese)

Huang Shisong, 1963: A study of the longitudinal movement and forecasting of subtropical anticyclones. *Acta Meteor. Sinica*, **33**(3), 320–332. (in Chinese)

Liu Yimin, Liu Hui, Liu Ping, et al., 1999a: The effect of spatially non-uniform heating on the formation and variation of subtropical high. Part II: Land surface sensible heating and East Pacific subtropical high. *Acta Meteor. Sinica*, **57**(4), 385–396. (in Chinese)

——, Wu Guoxiong, Liu Hui, et al., 1999b: The effect of spatially nonuniform heating on the formation and variation of subtropical high. Part III: Condensation heating and South Asian high and western Pacific subtropical high. *Acta Meteor. Sinica*, **57**(5), 525–538. (in Chinese)

—— and Wu Guoxiong, 2000: Reviews on the study of the subtropical anticyclone and new insight on some fundamental problems. *Acta Meteor. Sinica*, **58**(4), 500–512. (in Chinese)

Lu Riyu, 2001: Interannual variability of the summertime North Pacific subtropical high and its relation to atmospheric convection over the warm pool. *J. Meteor. Soc. Japan*, **79**(3), 771–783.

——, 2002: Indices of the summertime western North Pacific subtropical high. *Adv. Atmos. Sci.*, **19**(6), 1004–1028.

Shu Tingfei and Luo Huibang, 2003: Abrupt change of the West Pacific subtropical high and its interannual variation during the later spring and early summer. *Journal of Tropical Meteorology*, **19**(1), 17–26. (in Chinese)

Wang Lijuan, Guan Zhaoyong, and He Jinhai, 2006: The position variation of the West Pacific subtropical high and its possible mechanism. *Journal of Tropical Meteorology*, **12**(2), 113–120.

——, ——, and ——, 2007: Features of the large-scale circulation for flash-flood-producing rainstorm over South China in June 2005 and its possible cause. *Journal of Nanjing Institute of Meteorology*, **30**(2), 145–152. (in Chinese)

Wen Min and He Jinhai, 2002: Ridge movement and potential mechanism of western Pacific subtropical high in summer. *Journal of Nanjing Institute of Meteorology*, **25**(2), 289–297. (in Chinese)

Wu Guoxiong and Liu Huanzhu, 1999a: Complete form of vertical vorticity tendency equation and slantwise vorticity development. *Acta Meteor. Sinica*, **57**(1), 1–15. (in Chinese)

——, Liu Yimin, and Liu Ping, 1999b: The effect of spatially nonuniform heating on the formation and variation of subtropical high. Part I: Scale analysis. *Acta Meteor. Sinica*, **57**(3), 257–263. (in Chinese)

—— and Chou Jifan, 2002: *Dynamical Causes for the Formation and Variation of Subtropical Highs*. Science Press, Beijing, 36–47.

Xiong Wenbing, Li Jiangnan, and Yao Cai, 2007: Analyzing continuous rainstorm in southern China in June 2005. *Journal of Tropical Meteorology*, **23**(1), 90–97. (in Chinese)

Yanai, M., S. Esbensen, and J. H. Chu, 1973: Determination of bulk properties of tropical cloud clusters from large-scale heat and source budgets. *J. Atmos. Sci.*, **30**(4), 611–627.